

A combined crossed beam and *ab initio* investigation on the reaction of carbon species with C₄H₆ isomers. I. The 1,3-butadiene molecule, H₂CCHCHCH₂(X¹A')

I. Hahndorf, H. Y. Lee,^{a)} A. M. Mebel, S. H. Lin,^{a)} Y. T. Lee,^{a)} and R. I. Kaiser^{b)}
*Institute of Atomic and Molecular Sciences, 1, Section 4, Roosevelt Road, 107 Taipei, Taiwan,
Republic of China*

(Received 24 March 2000; accepted 11 July 2000)

The reaction between ground state carbon atoms, C(³P_j), and 1,3-butadiene, H₂CCHCHCH₂, was studied at three averaged collision energies between 19.3 and 38.8 kJmol⁻¹ using the crossed molecular beam technique. Our experimental data combined with electronic structure calculations show that the carbon atom adds barrierlessly to the π-orbital of the butadiene molecule via a loose, reactantlike transition state located at the centrifugal barrier. This process forms vinylcyclopropylidene which rotates in a plane almost perpendicular to the total angular momentum vector **J** around its C-axis. The initial collision complex undergoes ring opening to a long-lived vinyl-substituted triplet allene molecule. This complex shows three reaction pathways. Two distinct H atom loss channels form 1- and 3-vinylpropargyl radicals, HCCCHC₂H₃(X²A'') and H₂CCCC₂H₃(X²A''), through tight exit transition states located about 20 kJmol⁻¹ above the products; the branching ratio of 1- versus 3-vinylpropargyl radical is about 8:1. A minor channel of less than 10% is the formation of a vinyl, C₂H₃(X²A'), and propargyl radical C₃H₃(X²B₂). The unambiguous identification of two C₅H₅ chain isomers under single collision has important implications to combustion processes and interstellar chemistry. Here, in denser media such as fuel flames and in circumstellar shells of carbon stars, the linear structures can undergo a collision-induced ring closure followed by a hydrogen migration to cyclic C₅H₅ isomers such as the cyclopentadienyl radical—a postulated intermediate in the formation of polycyclic aromatic hydrocarbons (PAHs). © 2000 American Institute of Physics. [S0021-9606(00)00338-X]

I. INTRODUCTION

The mechanisms to form polycyclic aromatic hydrocarbons (PAHs) and ultimately soot in oxygen-poor combustion flames as well as outflow of carbon stars are of fundamental importance to the combustion community as well as for astrophysics. The relevance is due to the potency of PAH isomers inducing mutations and cancer together with the soot-enhanced entry of PAHs in the human respiratory system.¹ In the interstellar medium, PAHs and their cations, anions, radicals, alkyl and oxygen substituted PAHs are thought to comprise 10% to 20% of the interstellar carbon in molecular form, and are suggested as a carrier of unidentified infrared bands (UIRs). In addition, PAH species could be responsible for some of the diffuse interstellar absorption bands (DIBs) covering the visible spectrum from 440 nm to the near infrared.²

Due to the crucial importance of PAH-like species, experimentally and theoretically well-defined mechanisms to synthesize PAHs and their precursors in various terrestrial and extraterrestrial gaseous environments have been investigated recently. As one result of experimental and kinetic

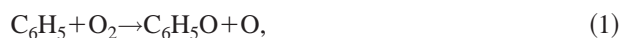
modeling studies of PAH formation in hydrocarbon flames³ the authors proposed that the origin of larger aromatics might be resonance-stabilized cyclopentadienyl radicals. In particular, a mechanism is proposed combining two or three cyclopentadienyl radicals, *c*-C₅H₅, followed by rearrangements to form naphthalene or phenanthrene molecules: both cyclopentadienyl radicals recombine first and then undergo H atom shifts and two H-atom ejections. Melius *et al.*⁴ supported this mechanism for the self-combination of cyclopentadienyl radicals by *ab initio* studies. The rate limiting step for this reaction is a 33.5±21.0 kJmol⁻¹ intrinsic barrier height attributed to the ejection of the first H-atom from the bicyclopentadiene adduct. The hydrogen shifts in the bicyclopentadienyl adduct occur fairly rapidly. Based on these considerations, the cyclopentadienyl radical combination may contribute as a possible reaction path to the PAH formation under the temperature conditions of circumstellar envelopes of hot carbon stars as well. In a recent investigation of sooting combustion flames⁵ this *c*-C₅H₅ radical is assumed to play a significant role in the reaction mechanism and is therefore included in the modeling of the combustion process. Despite this assumption the experimental confirmation still remains. There is no evidence given which isomer of the C₅H₅ radical mainly contributes to combustion processes. Supported by *ab initio* calculations, Lin *et al.* suggested a possible reaction path for the formation of *c*-C₅H₅ initiated by the phenyl radical which itself is formed via activation of benzene by abstraction of a hydrogen atom.⁶

^{a)}Also at Department of Chemistry, National Taiwan University, Taipei, 107, Taiwan, Republic of China.

^{b)}Author to whom correspondence should be addressed. Also with Department of Physics, National Taiwan University, Taipei, 107; and Department of Physics, Technical University Chemnitz, 09107 Chemnitz, Germany. Electronic mail: kaiser@po.iam.sinica.edu.tw

TABLE I. Experimental beam conditions and 1σ errors averaged over the experimental time: peak velocity v_p , speed ratio S (Ref. 36), peak collision energy, E_{coll} , center-of-mass angle, $\theta_{\text{C.M.}}$, composition of the carbon beam, and flux factor $f_v = n(\text{C}) * n(\text{H}_2\text{CCHCH}_2) * v_r$, in relative units, with the number density of the i th reactant n_i and the relative velocity v_r .

Beam	v_p (ms ⁻¹)	S	E_{coll} (kJmol ⁻¹)	$\theta_{\text{C.M.}}$	C ₁ :C ₂ :C ₃	f_v
C(³ P _j)	1800±10	7.2±0.2	19.3±0.3	62.5±0.4	1:0.3:0.7	1.0
C(³ P _j)	2260±20	7.2±0.2	28.0±0.5	56.9±0.3	1:0.2:0.8	1.3±0.2
C(³ P _j)	3000±50	6.9±0.2	38.8±1.4	49.0±0.4	1:0.2:0.8	1.6±0.3
C ₄ H ₆	770±10	9.2±0.2



However, no reliable experimental information is available on the mechanism of $c\text{-C}_5\text{H}_5$ radical formation. Therefore, we launched a systematic program to study alternative reaction pathways and investigate the atom-neutral reaction of C(³P_j) with distinct C₄H₆ isomers. Here, we unravel the chemical dynamics on the reaction of atomic carbon with 1,3-butadiene, H₂CCHCHCH₂. Although atomic carbon is only a minor species in oxidative flames, it is assumed to contribute significantly to combustion chemistry.⁷ C₄H₆ isomers have been observed in hydrocarbon flames, and about 90% of the C₄H₆ products are 1,3-butadiene.⁸ Various crossed beam reactions of atomic carbon with unsaturated hydrocarbon molecules demonstrated explicitly that these reactions are dominated by a carbon versus hydrogen exchange to form highly unsaturated, hydrogen-deficient hydrocarbon radicals. Therefore, our title reaction is strongly expected to synthesize C₅H₅ isomers.

II. EXPERIMENTAL SETUP

The experiments were performed under single-collision conditions using a universal crossed molecular beams apparatus described in Ref. 9 in detail. Briefly, a pulsed supersonic carbon beam was generated via laser ablation of graphite at 266 nm.¹⁰ The 30 Hz, 30–40 mJ output of a Spectra Physics GCR-270-30 Nd:YAG laser was focused onto a rotating carbon rod, and the ablated species were seeded into a pulse of neat helium gas at 4 atm backing pressure. A four-slot chopper wheel mounted after the ablation zone selected a 9.0 μs segment of the seeded carbon beam. Table I compiles the experimental beam conditions. The carbon beam and a pulsed 1,3-butadiene beam hold at 820±5 torr backing pressure passed through skimmers and crossed at 90° in the interaction region of the scattering chamber. To elucidate the position of the H atom loss, we performed experiments with partially deuterated 1,1,4,4-tetradeuterium-1,3-butadiene, D₂CCHCHCD₂. Reactively scattered products were detected in the plane defined by two beams using a rotatable detector consisting of a Brink-type electron-impact ionizer,¹¹ quadrupole mass filter, and a Daly ion detector at laboratory angles in 2.5° and 5.0° steps between 3.0° and 72.0° with respect to the primary beam. The velocity distribution of the products was recorded using the time-of-flight (TOF) technique, and information on the chemical dynamics of the reaction was gained by fitting the TOF spectra and the product angular

distribution in the laboratory frame (LAB) using a forward-convolution routine.¹² This approach initially assumes an angular flux distribution $T(\theta)$ and the translational energy flux distribution $P(E_T)$ in the center-of-mass system (C.M.). Laboratory TOF spectra and the laboratory angular distributions were then calculated from these $T(\theta)$ and $P(E_T)$ averaged over the apparatus and beam functions. Best TOF and laboratory angular distributions were archived by refining adjustable $T(\theta)$ and $P(E_T)$ parameters. The final outcome is the generation of a product flux contour map which reports the differential cross section, $I(\theta, u) \sim P(u) * T(\theta)$, as the intensity as a function of angle θ and product center-of-mass velocity u . Hence this map serves as an image of the reaction and contains all the information of the scattering process.

III. ELECTRONIC STRUCTURE AND RRKM CALCULATIONS

The geometries of the reactants, products, various intermediates, and transition states for the title reaction were optimized using the hybrid density functional B3LYP method, i.e., Becke's three-parameter nonlocal exchange functional¹³ with the nonlocal correlation functional of Lee, Yang, and Parr,¹⁴ and the 6-311G(d,p) basis set.¹⁵ Vibrational frequencies, calculated at the B3LYP/6-311G(d,p) level, were used for characterization of stationary points and zero-point energy (ZPE) correction. All the stationary points were positively identified for minimum or transition state. In some cases, geometries and frequencies were recalculated at the MP2/6-311G(d,p) and CCSD(T)/6-311G(d,p) levels.¹⁶

In order to obtain more reliable energies, we used the G2M(RCC,MP2)¹⁷ method, a modification of the Gaussian-2 [G2(MP2)] approach.¹⁸ The total energy in G2M(RCC,MP2) is calculated as follows:

$$\begin{aligned} E[\text{G2M(RCC,MP2)}] = & E[\text{RCCSD(T)/6-311G}(d,p)] \\ & + \Delta E(+3df2p) + \Delta E(\text{HLC}) \\ & + \text{ZPE}[\text{B3LYP/6-311G}(d,p)], \end{aligned} \quad (3)$$

where

$$\begin{aligned} \Delta E(+3df2p) = & E[\text{MP2/6-311+G}(3df,2p)] \\ & - E[\text{MP2/6-311G}(d,p)] \end{aligned} \quad (4)$$

and the empirical "higher level correction"

$$\Delta E(\text{HLC}) = -5.25n_\beta - 0.19n_\alpha, \quad (5)$$

where n_α and n_β are the numbers of α and β valence electrons, respectively. It has been shown that the G2M(RCC,MP2) method gives the averaged absolute deviation of 4.8 kJmol^{-1} of calculated atomization energies from experiment for 32 first-row G2 test compounds. The GAUSSIAN 94,¹⁹ MOLPRO 96,²⁰ and ACES-II²¹ programs were employed for the potential energy surface computations. In this article, we present only those results necessary to understand our experimental data. All details are given in a forthcoming publication.²²

We used the Rice–Ramsperger–Kassel–Marrus (RRKM) theory²³ for computations of rate constants of individual reaction steps. Rate constant $k(E)$ at a collision energy E for a unimolecular reaction $A^* \rightarrow A^\ddagger \rightarrow P$ can be expressed as

$$k(E) = \frac{\sigma}{h} \cdot \frac{W^\ddagger(E - E^\ddagger)}{\rho(E)}, \quad (6)$$

where σ is a symmetry factor, $W^\ddagger(E - E^\ddagger)$ denotes the total number of states for the transition state (activated complex) A^\ddagger with a barrier E^\ddagger , $\rho(E)$ represents the density of states of the energized reactant molecule A^* , and P is the product or products. The saddle point method was applied to evaluate $\rho(E)$ and $W(E)$.²³

IV. RESULTS

A. Reactive scattering signal

We observed reactive scattering signals at mass-to-charge ratios $m/e = 65$ to 60 , i.e., C_5H_5^+ (65) to the bare carbon cluster C_5^+ (60, Figs. 1–6). The relative intensity ratios of m/e 65:64:63:62:61:60 are 0.26:0.32:1.0:0.52:0.38:0.13 recorded at an electron energy of 200 eV; errors are within 10%. All TOF spectra could be fit with identical center-of-mass functions. Therefore, the signal at lower m/e ratios originates in the cracking of the C_5H_5^+ parent in the ionizer. Hence, we selected the most intense mass-to-charge ratio and took our data at $m/e = 63$. We like to point out that no radiative association to C_5H_6 ($m/e = 66$) could be detected. In the case of partially deuterated 1,3-butadiene, $\text{D}_2\text{CCHCHCD}_2$, we recorded TOF spectra at the center-of-mass angles, and took data at $m/e = 69$ ($\text{C}_5\text{D}_4\text{H}^+$), 68 (C_5D_4^+ and/or $\text{C}_5\text{D}_3\text{H}_2^+$), 67 ($\text{C}_5\text{D}_3\text{H}^+$), and 66 (C_5D_3^+ and/or $\text{C}_5\text{D}_2\text{H}_2^+$).²⁴ This indicates that at least the C versus H exchange channel to form $\text{C}_5\text{D}_4\text{H}$ exists. Since $m/e = 68$ can originate from fragmentation of $m/e = 69$ in the detector or from D atom loss, we cannot resolve at the present stage if a D atom emission occurs. To tackle this question, we have to fit the TOF spectra at $m/e = 69$ and 68, cf. Sec. IV B.

B. Laboratory angular distributions (LAB) and TOF spectra

The most probable Newton diagrams of the title reaction as well as the laboratory angular (LAB) distributions of the C_5H_5 product are displayed in Figs. 1–3 collision energies of 19.3, 28.0, and 38.8 kJmol^{-1} , respectively. At each collision energy, the LAB distribution peaks close to the CM angles, cf. Table I. This suggests that the reaction proceeds via indirect reactive scattering dynamics through long-lived C_5H_6

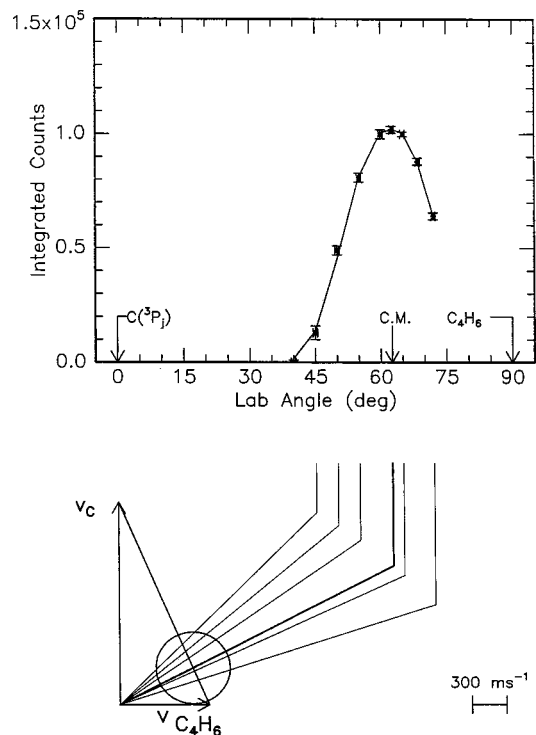


FIG. 1. Lower: Newton diagram for the reaction $\text{C}(^3\text{P}_j) + \text{H}_2\text{CCHCHCH}_2(X^1\text{A}')$ at a collision energy of 19.3 kJmol^{-1} . The circle stands for the maximum center-of-mass recoil velocity of the C_5H_5 isomer assuming no energy channels into the internal degrees of freedom. Upper: Laboratory angular distribution of product channel at $m/e = 63$. Circles and 1σ error bars indicate experimental data, the solid lines the calculated distribution. C.M. designates the center-of-mass angle. The solid lines originating in the Newton diagram point to distinct laboratory angles whose TOFs are shown in Fig. 4.

complex(es) holding a lifetime exceeding the(ir) rotational period(s). In addition, all LAB distributions are very broad and extend to about 45.0° in the scattering plane defined by both beams. This data and the $\text{C}_5\text{H}_5 + \text{H}$ product mass ratio of 65 hint that the center-of-mass translational energy distributions $P(E_T)$'s peak away from zero.

C. Center-of-mass translational energy distributions, $P(E_T)$

Figure 7 shows best fits of the translational energy distributions $P(E_T)$. Both the LAB distributions and TOF data could be fitted with one $P(E_T)$ extending to a maximum translational energy release E_{max} of 205, 230, and 250 kJmol^{-1} , respectively. These high-energy cutoffs are accurate within 10 kJmol^{-1} . In the most favorable case the energetics of the product isomers are well separated. Then E_{max} , i.e., the sum of the reaction exothermicity and relative collision energy, can be utilized to identify individual C_5H_5 isomers. Correcting for the collision energy shows that our reaction is exothermic by about $214 \pm 15 \text{ kJmol}^{-1}$. In addition, all $P(E_T)$'s peak away from zero and show distribution maxima of 30–50 kJmol^{-1} . In the case of partially deuterated butadiene (Fig. 8), the TOF at $m/e = 69$ could be fit with kinematics of a H atom loss and a single $P(E_T)$ showing identical pattern as the translational energy distribution of 1,3-butadiene. However, at $m/e = 68$, two contributions of a

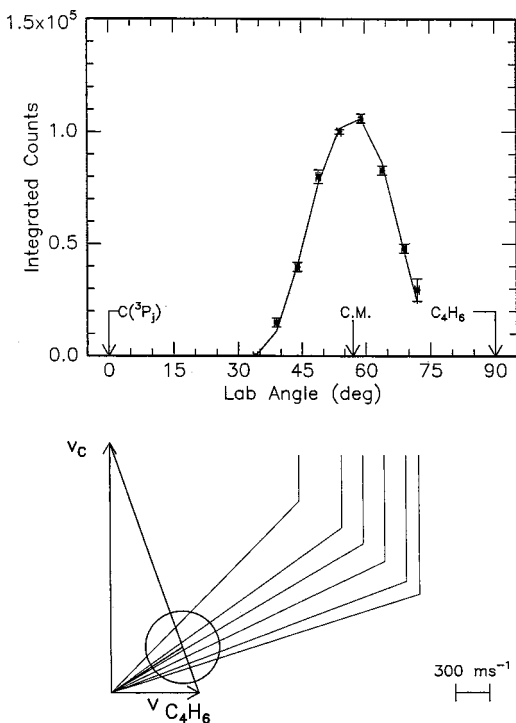


FIG. 2. Lower: Newton diagram for the reaction $C(^3P_j) + H_2CCHCHCH_2(X^1A')$ at a collision energy of 28.0 kJmol^{-1} . The circle stands for the maximum center-of-mass recoil velocity of the C_5H_5 isomer assuming no energy channels into the internal degrees of freedom. Upper: Laboratory angular distribution of product channel at $m/e=63$. Circles and 1σ error bars indicate experimental data, the solid lines the calculated distribution. C.M. designates the center-of-mass angle. The solid lines originating in the Newton diagram point to distinct laboratory angles whose TOFs are shown in Fig. 5.

D atom loss ($C_5D_3H_2^+$) and fragmentation of the H atom loss isomer to $C_5D_4^+$ are crucial to get a reasonable fit of the data. These results show clearly the formation of at least two distinct C_5H_5 isomers.

D. Center-of-mass angular distributions, $T(\theta)$, and flux contour maps $I(u, \theta)$

At all collision energies the $T(\theta)$ s are isotropic and symmetric around $\pi/2$. This implies that either the lifetime of the decomposing C_5H_6 complex(es) is(are) longer than its rotational period τ_r , or that two hydrogen atoms of the intermediate can be interconverted through a rotational axis.²⁵ In this case, the light H atom could be emitted in θ and $\theta-\pi$ to result for the forward-backward symmetry of $T(\theta)$. We like to point out that at the highest collision energy, a slightly backward scattered $T(\theta)$ up to $I(180^\circ)/I(0^\circ)=1.05$ can fit the data as well. Due to the light H atom emission, these isotropic angular distributions are the result of a poor coupling between the initial and final angular momentum vectors, \mathbf{L} and \mathbf{L}' , respectively, as already observed in crossed beams reaction of atomic carbon with methylacetylene,²⁶ allene,²⁷ benzene,²⁸ and propylene.²⁹ Since angular momentum has to be conserved, a large fraction of the initial orbital angular momentum must therefore be routed into rotational excitation of the C_5H_5 reaction products. Figure 9 shows both two- and three-dimensional center-of-mass flux contour

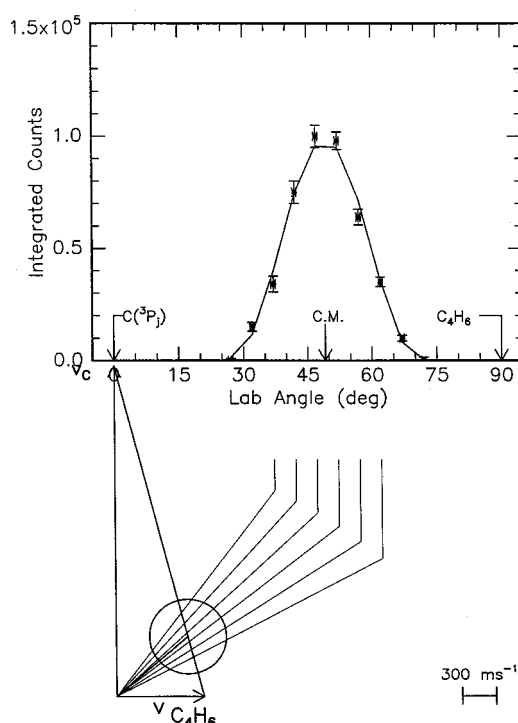


FIG. 3. Lower: Newton diagram for the reaction $C(^3P_j) + H_2CCHCHCH_2(X^1A')$ at a collision energy of 38.8 kJmol^{-1} . The circle stands for the maximum center-of-mass recoil velocity of the C_5H_5 isomer assuming no energy channels into the internal degrees of freedom. Upper: Laboratory angular distribution of product channel at $m/e=63$. Circles and 1σ error bars indicate experimental data, the solid lines the calculated distribution. C.M. designates the center-of-mass angle. The solid lines originating in the Newton diagram point to distinct laboratory angles whose TOFs are shown in Fig. 6.

plots $I(\theta, E_T)$; since all translational energy distributions look very similar, we show only data at the lowest collision energy as a typical example. As we can expect from the center-of-mass angular distribution, the best-fit data show a forward-backward symmetric flux profile. Integrating the $I(\theta, E_T)$ s at each collision energy and correcting for the reactant flux as well as relative reactant velocity, we find an integrated relative reactive scattering cross section ratio of $\sigma(19.3 \text{ kJmol}^{-1})/\sigma(28.0 \text{ kJmol}^{-1})/\sigma(38.8 \text{ kJmol}^{-1})=1.0:0.7 \pm 0.2:0.5 \pm 0.1$ within our error limits. Therefore, the cross section slightly rises as the collision energy decreases. This result together with recent kinetic data³⁰ and our electronic structure calculations, cf. Sec. V, suggest that the reaction has no entrance barrier.

V. DISCUSSION

A. The C_5H_6 potential energy surface

1. Addition to one C=C double bond

Our electronic structure calculation shows that 1,3-butadiene can exist in a trans and cis form; the latter is energetically less favored by 12 kJmol^{-1} ; both isomers can be inter-converted via a 23.5 kJmol^{-1} high barrier. The transition state of this process depicts a C-C bond distance increasing slightly from 146 pm (trans) via 149 pm (transition state) to 147 pm. Due to the enhanced repulsive interaction, the cis isomer shows no symmetry at all whereas the trans

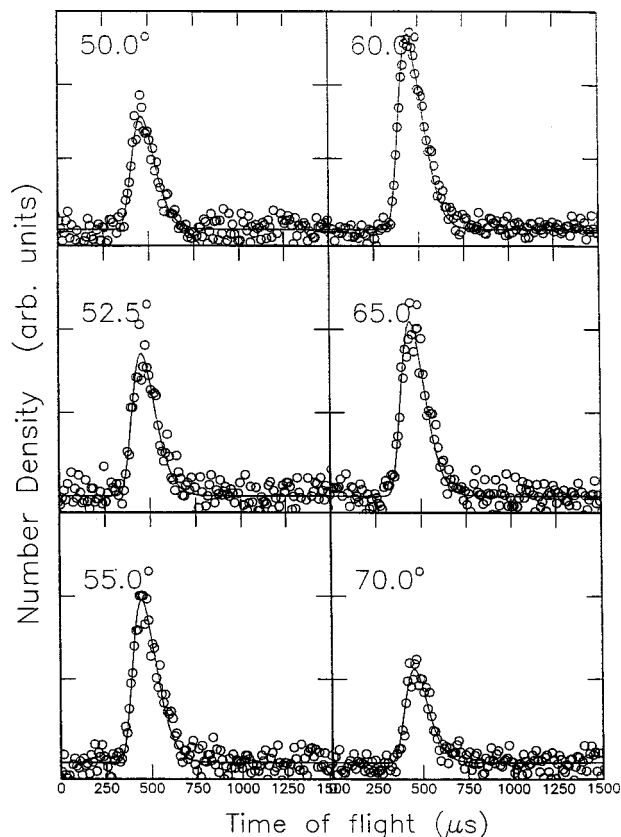


FIG. 4. Time-of-flight data at $m/e=63$ for indicated laboratory angles at a collision energy of 19.3 kJmol^{-1} . Open circles represent experimental data, the solid line represents the fit.

form belongs to the C_s point group. In this section, we discuss first the reaction of atomic carbon with the trans isomer. Here, $C(^3P_j)$ can add barrierlessly to the carbon-carbon double bond forming a vinyl-substituted triplet cyclopropylidene radical **i1**, Figs. 10 and 11. The latter is bound by 213 kJmol^{-1} with respect to the separated reactants and exists in two nearly isoenergetic cis and trans forms (**i1-cis** and **i1-trans**). We mention that the carbon additions to trans and cis 1,3-butadiens give **i1-trans** and **i1-cis**, respectively. The conformers of **i1** are expected to readily rearrange to each other by rotation around the single C-C bond with a low barrier.

i1 can undergo a [1,2] or [1,3] hydrogen shift via 200 kJmol^{-1} barriers (pathway 1 and 2) or a ring opening (pathway 3). The first two pathways form the **i3** (cis/trans) and the **i4** isomers (cis/trans), respectively. Compared to atomic carbon and 1,3-butadiene, **i3** and **i4** are 250 and 196 kJmol^{-1} more stable. No symmetry element exists; both isomers represent vinyl-substituted triplet cyclopropene molecules. A final hydrogen loss can form the C_3H_5 isomers **p3-p6** (from **i3**) and **p6-p11** (from **i4**). The optimized product geometries are shown in Fig. 12. Among these isomers, **p6** is the most stable structure since the aromatic vinylcyclopropenyl radical is formed. The energy difference to the more stable vinylpropargyl radicals of about 110 kJmol^{-1} corresponds very well as found in the unsubstituted products propargyl and cyclopropenyl ($100 \pm 25 \text{ kJmol}^{-1}$). Structures **p3**, **p4**, **p7**, and **p8** represent less stable, substituted cyclopropene molecules formed via H atom loss from the vinyl group. The remaining

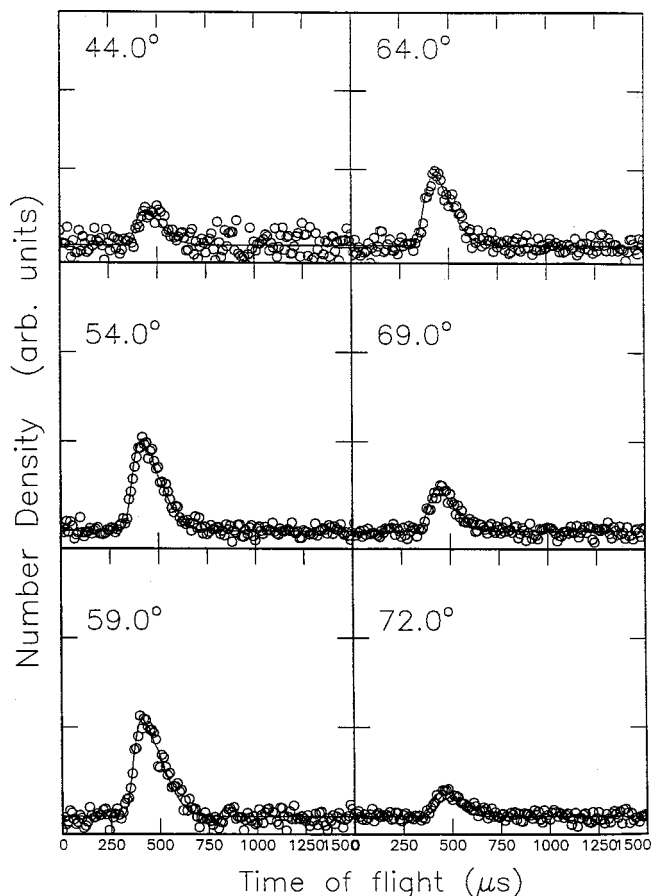


FIG. 5. Time-of-flight data at $m/e=63$ for indicated laboratory angles at a collision energy of 28.0 kJmol^{-1} . Open circles represent experimental data, the solid line represents the fit.

isomers **p5**, **p10**, and **p11** can be visualized as derivatives of cyclopropen-2-yl in which one H atom is replaced by a C_2H_3 group. Compared to the hydrogen migration pathways, the ring opening of **i1** (pathway 3) involves a much lower barrier of only 51 kJmol^{-1} . This process yields a vinyl substituted triplet allene diradical **i5** (trans) which is about 147 kJmol^{-1} more stable than **i1**.

The **i5** intermediate can undergo a trans-cis isomerization to **i5** (cis) followed by a [1,2] hydrogen shift to give **i8** which is almost isoenergetic to **i5** (cis). The barrier for this process is about 200 kJmol^{-1} —identical to those H shifts in **i1**. A subsequent ring closure via a 78 kJmol^{-1} barrier leads to triplet cyclopentadiene **i6**—the global minimum of the triplet C_5H_6 potential energy surface (PES). Another pathway from **i5** (cis) to **i6** involves ring closure to **i9** with a barrier of 108.0 kJmol^{-1} followed by a [1,2] hydrogen shift in the ring with a barrier of 216.0 kJmol^{-1} . **i6** can fragment via C-H bond cleavages to form the cyclopentadienyl radical **p16** which represents the global minimum of the C_5H_5 PES. Here, the theoretically derived exothermicity of 332 kJmol^{-1} is in excellent agreement with thermodynamical data predicting 323 kJmol^{-1} .³¹

Alternative H atom loss channels to **p17** and **p18** are less favorable by about 140 kJmol^{-1} . In these systems, the resonance stabilization is less pronounced as compared to the cyclopentadienyl radical **p16**. Besides the cis-trans isomer-

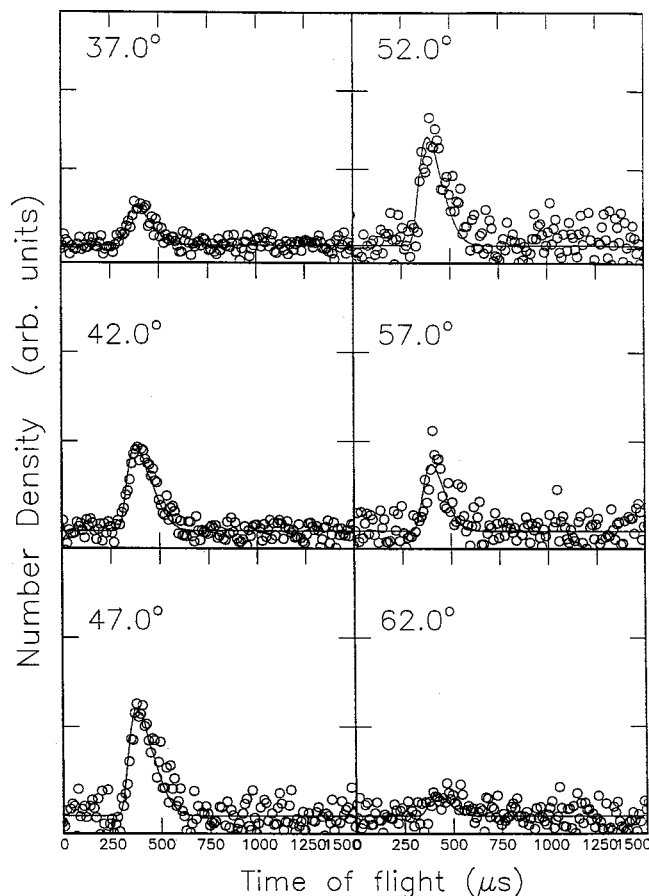


FIG. 6. Time-of-flight data at $m/e=63$ for indicated laboratory angles at a collision energy of 38.8 kJmol^{-1} . Open circles represent experimental data, the solid line represents the fit.

ization, **i5-trans** can decompose via C–H bond cleavage to four distinct C₅H₅ isomers **p12–p15**. Here, tight exit transition states located about 20 kJmol^{-1} above the products lead vinyl-substituted propargyl radicals, i.e., 1- and 3-vinylpropargyl radicals, HCCCH–C₂H₃ (**p14**), H₂CCC–C₂H₃ (**p15**).

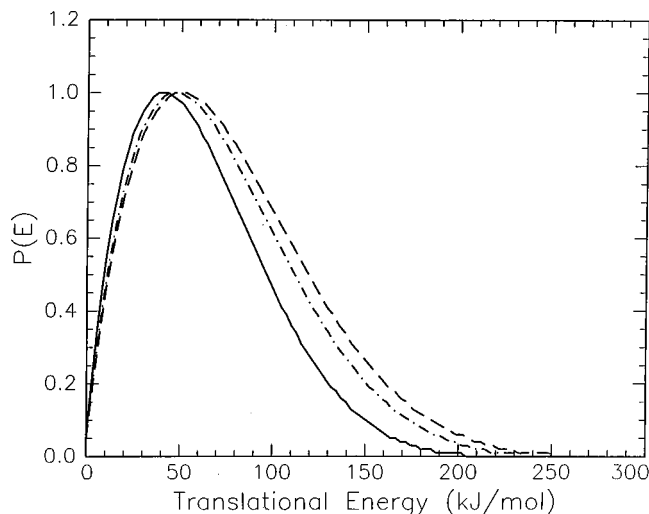
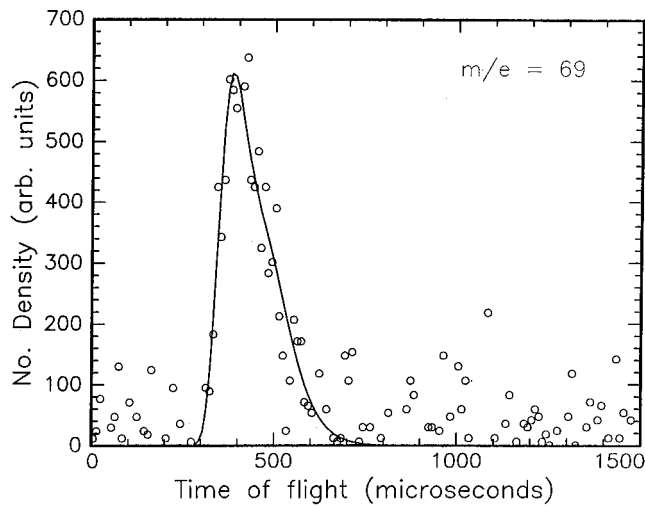
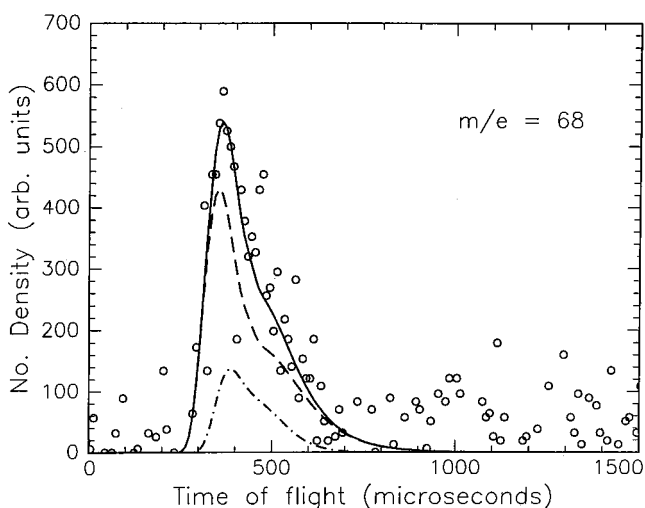


FIG. 7. Center-of-mass translational energy flux distributions for the reaction $\text{C}(^3\text{P}_j) + \text{H}_2\text{CCHCHCH}_2(X^1A')$ at collision energies of 19.3 (solid line), 28.0 (dashed-dotted line), and 38.3 kJmol^{-1} (dashed line).



(a)



(b)

FIG. 8. Time-of-flight data of $m/e=69$ (top) and 68 (bottom) at the center-of-mass angle recorded at a collision energy of 38.8 kJmol^{-1} . Experimental data are indicated by open circles. At $m/e=69$, the solid line represents the best fit of the H atom loss channel; at $m/e=68$ best fits are indicated by dashed line (D atom loss), dashed-dotted line (H atom loss channel), and solid line (sum of both contribution).

The reaction exothermicities of these processes are calculated to be 210 and 192 kJmol^{-1} , respectively. The stability sequence can be rationalized in terms of an enhanced delocalization of the unpaired electron in **p14** (increased delocalization incorporating the C₂H₃ group) compared to **p15**. The energetics to form substituted allene radicals **p12** and **p13** are less favorable and are only exothermic by 125 and 94 kJmol^{-1} . We like to point out that we were unable to find an exit transition state from **i5** to **p12**+H. Both at the B3LYP/6-31G** and MP2/6-311G** levels of theory the transition state optimization converged to the separated products indicating that the exit barrier does not exist. **i5-trans** can also dissociate to the vinyl and propargyl radicals by splitting the C–C bond with a barrier of 219.6 kJmol^{-1} . The exit barrier in this case is 25.5 kJmol^{-1} and the total reaction exothermicity is 165.7 kJmol^{-1} , i.e., lower than those for **p14** and **p15** but significantly higher than for **p12** and **p13**.

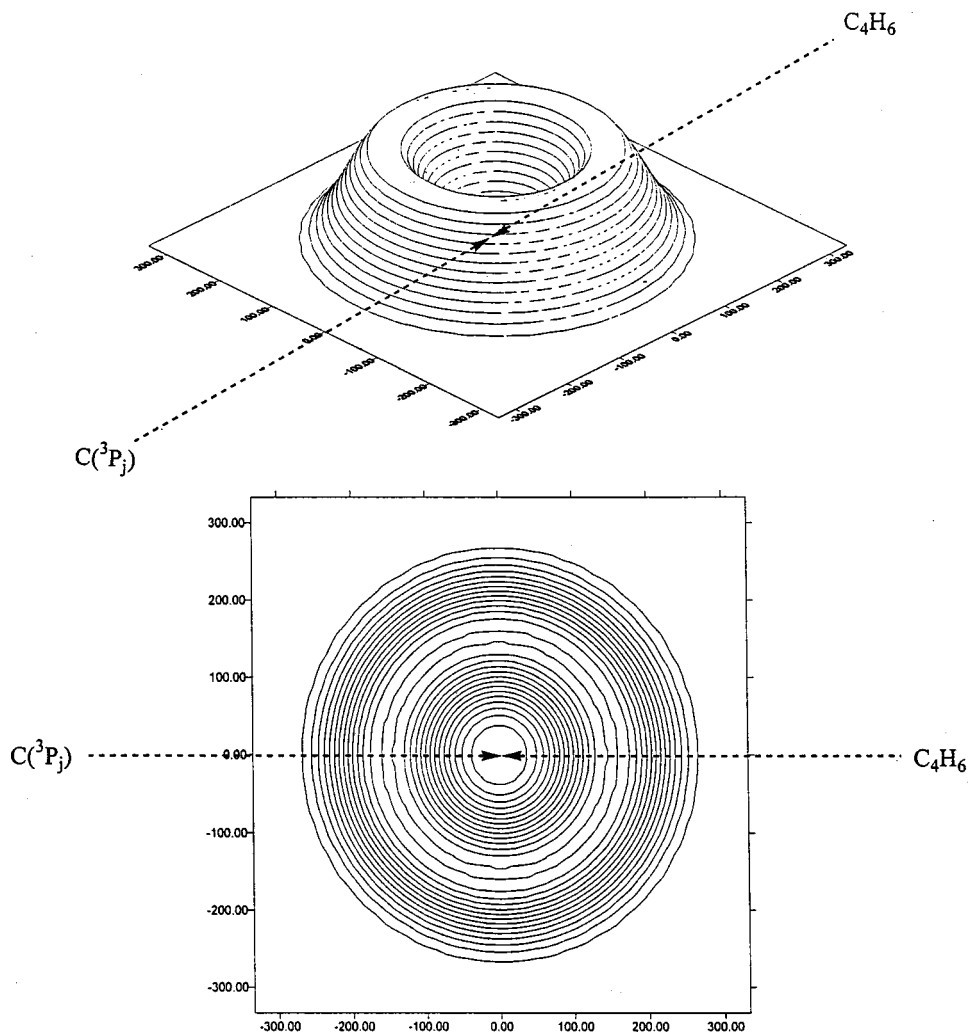


FIG. 9. Contour flux map for the reaction $C(^3P_j) + H_2CCHCHCH_2(X^1A')$ at a collision energy of 19.3 kJmol^{-1} . (a) Three-dimensional map, (b) two-dimensional projection. Units are given in ms^{-1} .

2. Addition to two C=C double bonds

If the 1,3-butadiene molecule reacts in its *cis* form with atomic carbon, $C(^3P_j)$ could attack both terminal carbon atoms simultaneously without entrance barrier under C_{2v} or C_s symmetry forming a pentacyclic triplet intermediate **i2**. The latter is stabilized by 341 kJmol^{-1} with respect to atomic carbon plus *trans* 1,3-butadiene and can either undergo H atom migration via a 184 kJmol^{-1} barrier to **i6** or fragments through a barrier located 10 kJmol^{-1} above the products to C_5H_5 isomer **p17**. The fate of **i6** was already outlined in the previous section.

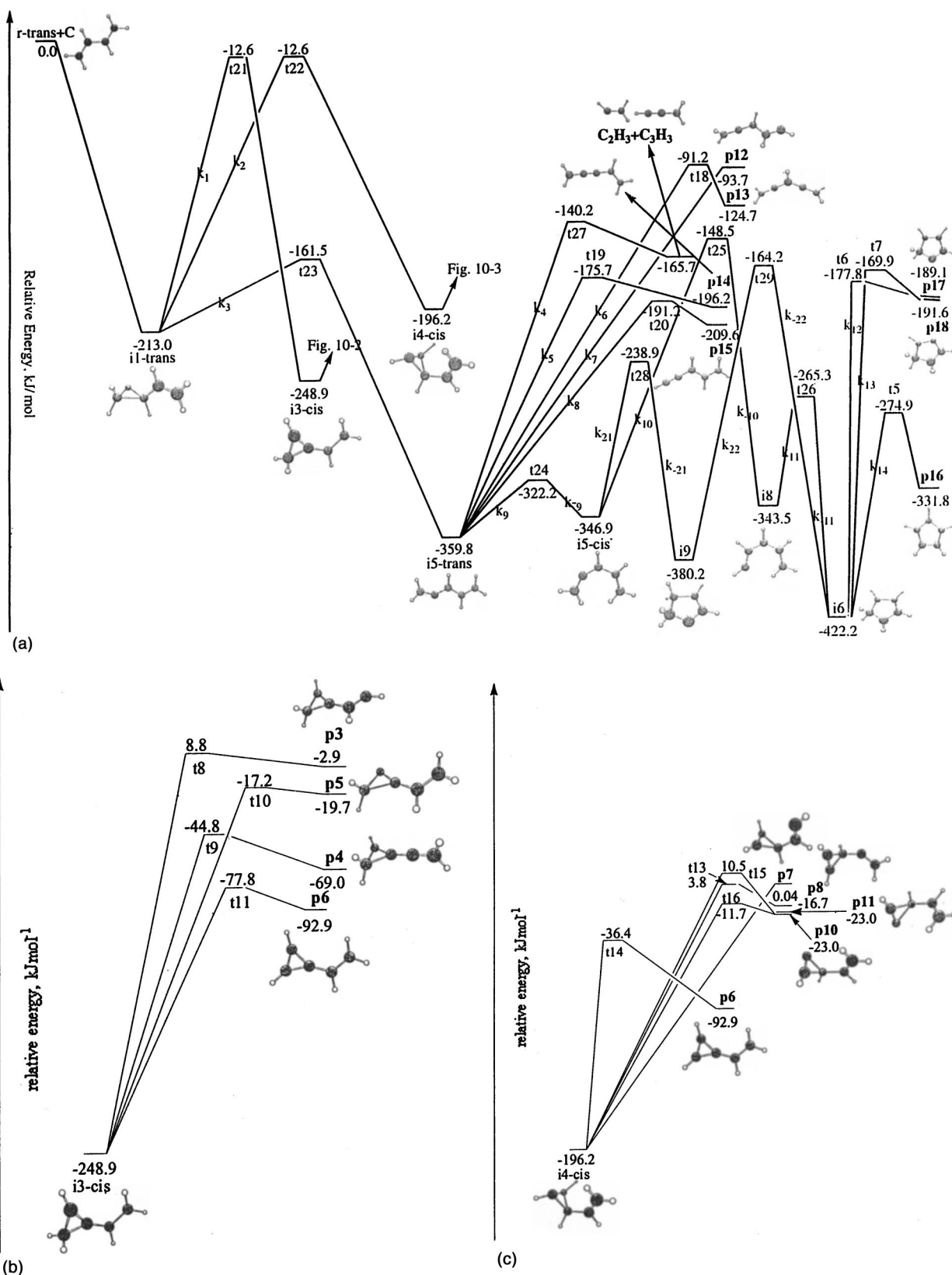
3. Insertion into C–H and C–C bonds

Despite a careful search, no transition states of a $C(^3P_j)$ insertion into C–H and C–C bonds could be found. We started the saddle point optimization from the geometries with a CCH three-membered ring suggesting that a C–H bond in 1,3-butadiene is broken and two new bonds, C–C and C–H, with the attacking carbon atom are formed during the insertion process. This process would lead directly to a $HCCHCHCH_2$ intermediate, a *trans* conformer of **i8**. However, the energies of the initial structures are very high. Upon the transition state search, the C–H bond in 1,3-butadiene is restored, and the system descends to the vicinity of

i1 or **i5**, indicating that the insertion pathway does not contain a first-order saddle point. Our finding strongly correlates with previous crossed beam experiments of $C(^3P_j)$ with unsaturated hydrocarbons acetylene,³² ethylene,³³ methylacetylene,²⁶ allene,²⁷ propylene,²⁹ benzene,²⁸ and the propargyl radical.³⁴ Here, only an addition to the π -electronic system was observed, but no symmetry forbidden insertion into C–H or C–C bonds.

B. Identification of reaction product(s)

The translational energy distributions show that the reaction to the C_5H_5 isomer(s) is exothermic by $215 \pm 15 \text{ kJmol}^{-1}$. If we compare this data with our electronic structure calculations, it is evident that the C_5H_5 isomers **p16**, **p17**, **p18** (from intermediate **i6**) or **p14** and **p15** (from intermediate **i5-trans**) contribute to the reactive scattering signal within the error limits. Since *trans* 1,3-butadiene is more than 99.4% in our secondary beam, the contribution of the *cis* isomer is marginally. An alternative pathway—a collision-induced *trans-cis* isomerization of 1,3-butadiene—is energetically feasible since even our lowest collision energy of 19.3 kJmol^{-1} can pass the isomerization barrier of 24 kJmol^{-1} . The reader has to keep in mind, however, that our experiments are performed under single-collision conditions;

FIG. 10. Schematic representation of the lowest energy pathways on the triplet C_3H_6 PES.

this means that upon cis-trans isomerization, no third body reaction partner to form **i2** is present, and hence this complex cannot be formed. **p17** and **p18** do not play a role in our experiments. Reaction to both isomers must proceed via **i6**

though H atom emission. If **i6** existed however, a C-H bond rupture is expected to proceed via the lowest energy pathway to cyclopentadienyl, **p16**. This conclusion gains strong support from our RRKM calculations: the ratios of the rate con-

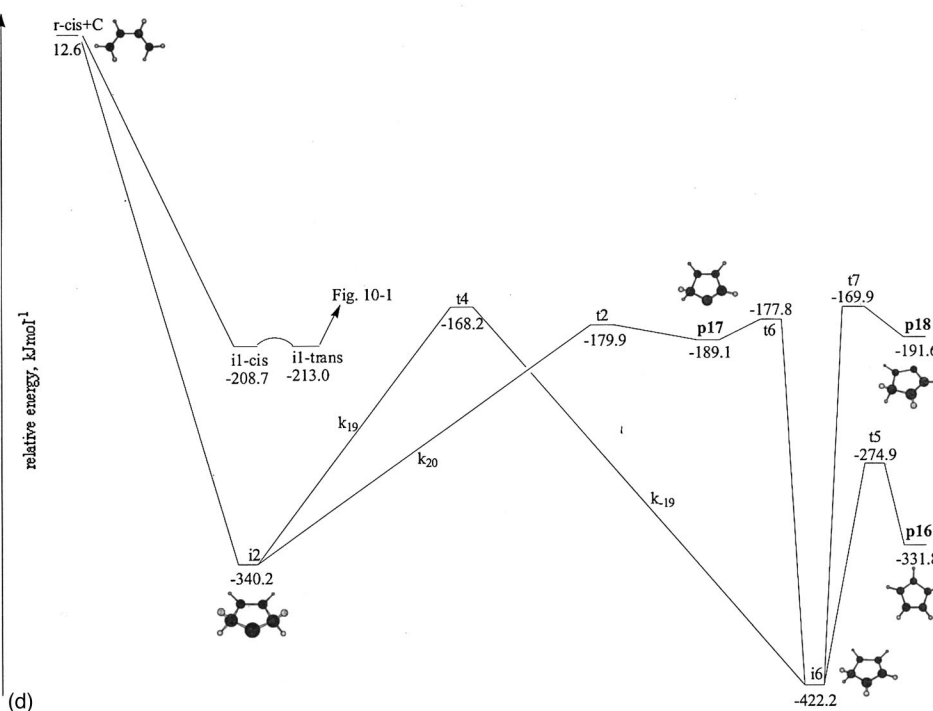
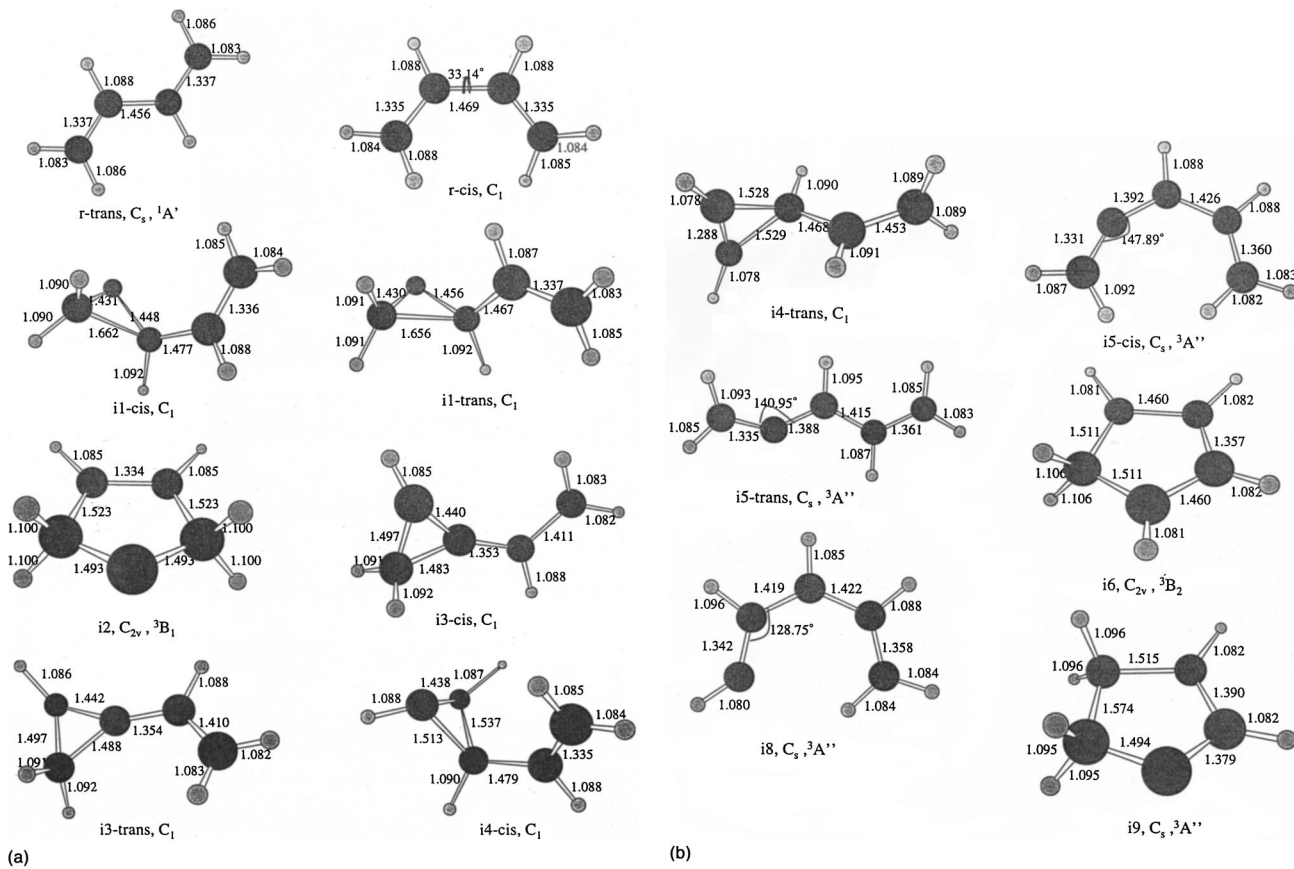


FIG. 10. (Continued.)

FIG. 11. Structures of potentially involved triplet C_5H_6 collision complexes. Bond lengths are given in Angstrom, bond angles in degrees.

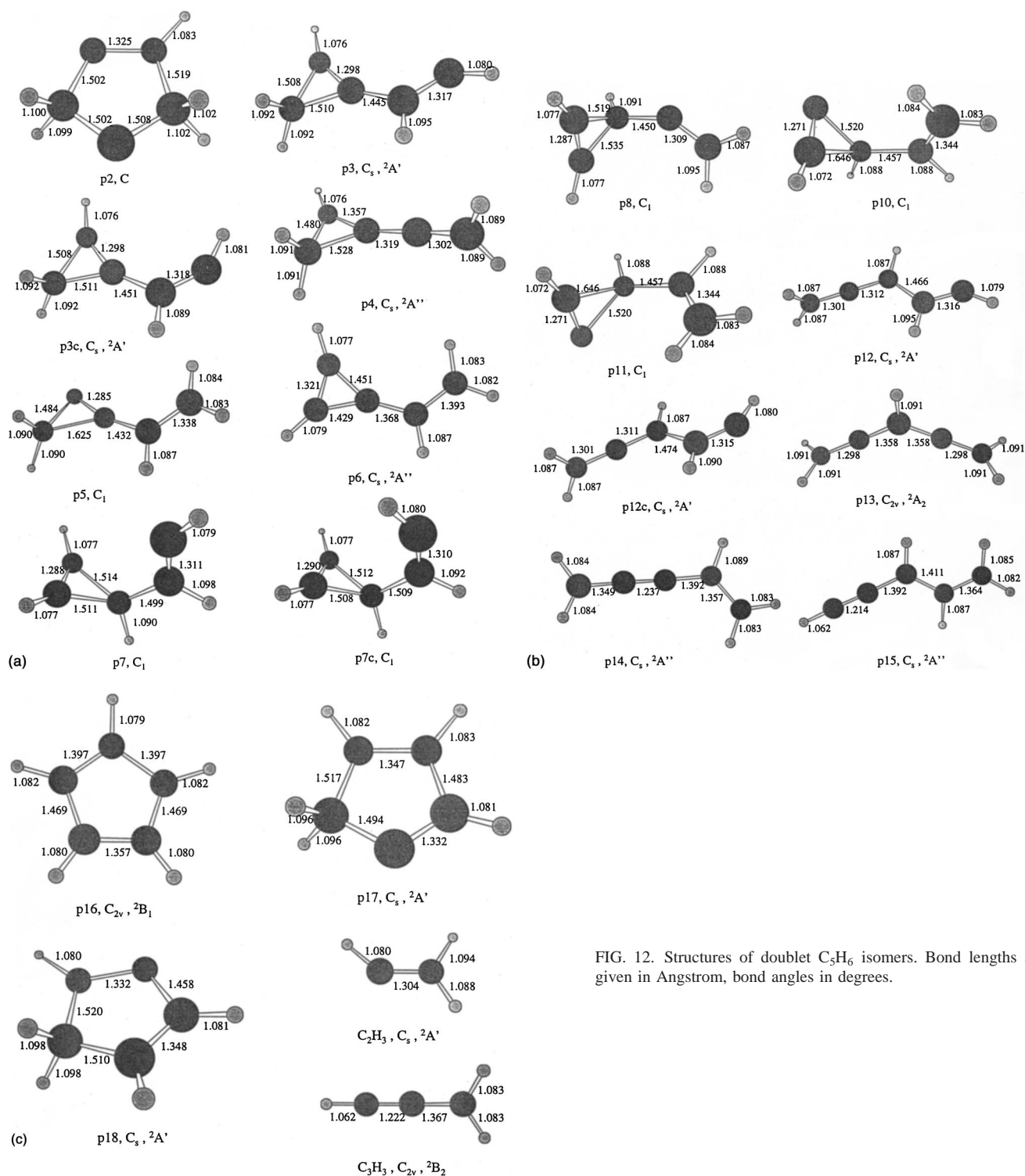


FIG. 12. Structures of doublet C₅H₆ isomers. Bond lengths are given in Angstrom, bond angles in degrees.

stants show $k(\mathbf{p16}):k(\mathbf{p18}):k(\mathbf{p17})=1:0.005:0.019$ (19.3 kJmol⁻¹), $k(\mathbf{p16}):k(\mathbf{p18}):k(\mathbf{p17})=1:0.007:0.022$ (28.0 kJmol⁻¹), and $k(\mathbf{p16}):k(\mathbf{p18}):k(\mathbf{p17})=1:0.008:0.027$ (38.8 kJmol⁻¹). Therefore, **p16** would be the dominate reaction product, and the reaction should be exothermic by 332 kJmol⁻¹. This is not supported by our experiments which suggest an exothermicity of 215 ± 15 kJmol⁻¹. We like to stress, however, that a long energy tail of our $P(E_T)$'s with $P(E)=0.01-0.03$ extending to 350 kJmol⁻¹ has no significant influence on our fit. Hence minor amounts of **p16** might

have been formed. This will be subject to RRKM studies, cf. Sec. V D. Based on these considerations, **p14** and **p15** are the only possible major reaction products which do confirm with the experimentally determined energetics of the reaction.

But is it feasible that less stable C₅H₅ isomers are formed as well to a minor amount? In principle, these isomers might be synthesized via C-H bond ruptures of reactive intermediates **i3**, **i4**, and **i5**. All three complexes, however, can only be formed through **i1**. The fate of the latter is governed by ring opening to **i5**. Compared to a 200 kJmol⁻¹

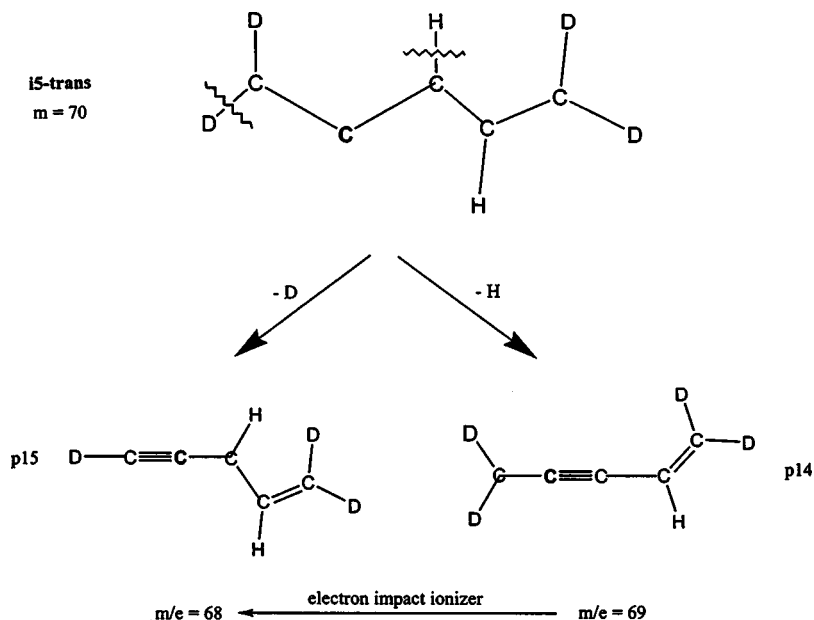


FIG. 13. Decomposition of the partially deuterated complex **i5-trans** to **p14** and **p15**.

barrier which must be passed to **i3** and **i4**, the barrier to **i5** is only 50 kJmol^{-1} and hence this pathway is the energetically most favorable one. Our RRKM investigation verifies this result as well, and the rate constants calculate to $k(\mathbf{i3}):k(\mathbf{i4}):k(\mathbf{i5}) = 7 \times 10^{-8}:1 \times 10^{-5}:1$ (19.3 kJmol^{-1}), $k(\mathbf{i3}):k(\mathbf{i4}):k(\mathbf{i5}) = 2 \times 10^{-7}:4 \times 10^{-5}:1$ (28.0 kJmol^{-1}), and $k(\mathbf{i3}):k(\mathbf{i4}):k(\mathbf{i5}) = 5 \times 10^{-7}:2 \times 10^{-4}:1$ (38.8 kJmol^{-1}). Therefore, **i1** reacts predominantly to **i5**, and **p3–p11** play no role in our reaction. **i5** decomposes via C–H rupture or undergoes ring closure, H shifts, and H atom emission. The latter process gives **p16**, which has not been observed as a major product in our crossed beam experiments. Based on these results, only **p12** and **p13** might resemble additional candidates. But since the exit barriers to form these isomers are about 105 kJmol^{-1} higher compared to those involved in a H atom emission to **p14** and **p15**, both **p12** and **p13** are negligible.

Our isotopic studies with partially deuterated 1,3-butadiene help to unravel the final question if **p14** or **p15**, or even both radicals are formed, cf. Fig. 13. Once **i5-trans** ($m = 70$) has been formed, only a H atom loss ($m/e = 69$) at the C3 atom goes hand in hand with the formation of **p14**; an alternative H loss at C4 would yield **p13**, which was eliminated earlier as a possible reaction product. In strong analogy, solely a D fragmentation of the C1–D bond is confirmed with the experimentally determined reaction energy of $215 \pm 15 \text{ kJmol}^{-1}$; and a C5–D loss would have formed unobserved **p12**. In conclusion, these isotopic studies combined with the energetics of the reaction confirm the formation of **p14** and **p15**. This experimental result is well supported by RRKM studies as well, and the ratios of the rate constants are $k(\mathbf{p13}):k(\mathbf{p14}):k(\mathbf{p15}) = 8 \times 10^{-6}:0.12:1$ (19.3 kJmol^{-1}), $k(\mathbf{p13}):k(\mathbf{p14}):k(\mathbf{p15}) = 1 \times 10^{-5}:0.13:1$ (28.0 kJmol^{-1}), and $k(\mathbf{p13}):k(\mathbf{p14}):k(\mathbf{p15}) = 1 \times 10^{-5}:0.13:1$ (38.8 kJmol^{-1}). Therefore, **p14** and **p15** are clearly identified as the reaction products. Obviously, **p13** does not play any role in the reactions.

C. The actual reaction pathway on the C_5H_6 potential energy surface

But what are the underlying dynamics to form the C_5H_5 isomers **p14** and **p15**? Based on our data, the chemical reaction dynamics are indirect and proceed via complex formation. In our molecular beam, more than 99.4% of the 1,3-butadiene exists in the energetically more stable trans form. Here, the singly occupied p_x and p_y orbitals of $\text{C}(^3P_j)$ can interact without entrance barrier perpendicular to the butadiene plane with the π orbital at the carbon–carbon double bond under C_1 symmetry on the 3A surface to form **i1-trans**, cf. Fig. 13. This approach supports a maximum orbital overlap to form two C–C– σ bonds in triplet vinyl cyclopropylidene. Since the butadiene molecules are prepared in a supersonic expansion, their rotational angular momentum is negligible, and the total angular momentum **J** is the initial orbital angular momentum **L**. Since $\mathbf{L} \approx \mathbf{J}$, **i1** rotates in a plane almost perpendicular to **L** around the *C* axis of the C_5H_6 isomer **i1**. A consecutive ring opening via a 50 kJmol^{-1} barrier conserves the rotational axis of the highly prolate triplet vinylallene complex **i5-trans** which has an asymmetry parameter $\kappa = -0.994$. The deep potential energy well of 360 kJmol^{-1} of **i5** explains the forward–backward symmetric center-of-mass angular distributions as found experimentally, and hence the decomposing **i5** complex has a lifetime longer than its rotation period around the *C* axis. An alternative explanation of a decomposing complex in which two hydrogen atoms can be interconverted through a rotation axis can be dismissed, since **i5** belongs to the C_1 point group. We like to stress that the reaction dynamics discussed so far are in line with large impact parameters leading to **i5** within orbiting limits. The contribution of large impact parameters which dominate the reaction was already mentioned in Sec. IV D. Our data suggest that the relative cross section rises as the collision energy decreases. Final C–H bond ruptures in **i5** yield the experimentally observed vinylpropargyl

radicals **p14** and **p15** rotating around their C axis. The isotopic studies show clearly that only those H atoms adjacent to the carbon atom close to the activated bonds formally inserted in the former carbon-carbon double bond are lost. No C–H or C5–H bond is broken. Further, both exit transition states to vinylpropargyl are tight and located about 20 kJmol^{-1} above the products; this gains support from our *ab initio* calculations showing imaginary frequencies of 588*i* and 561*i* cm^{-1} , respectively. The characteristics of both transition states are consistent with the reversed reaction of a H atom addition to an unsaturated olefinic or acetylenic system which has similar orders of magnitude of the entrance barriers as observed in our experiments. In addition, the indirect scattering dynamics of the title reaction are supported by a small fraction of 30%–35% of total available energy channeling into translation as already observed in a similar complex forming reaction of atomic carbon with unsaturated hydrocarbons as studied in our group.

These considerations show clearly that the reaction of atomic carbon with *trans* 1,3-butadiene is not thermodynamically controlled since the most stable cyclopentadienyl radical **p16** is not a major product. The formation of 1- and 3-vinylpropargyl is a direct consequence of the involved PES and the transition state choking the H atom migration from **i5-cis** to **i8**. A similar case in which the reaction was not controlled thermodynamically was found in the $C(^3P_j)/C_6H_6$ system in which the thermodynamically less stable 1,2-didehydrocycloheptatrienyl isomer was formed.

D. RRKM Calculations

Our experimental data alone cannot identify the contribution of the cyclopropenyl radical, **p16**. Further, we investigate the experimentally not observed C_2H_3 elimination from **i5**. To solve this problem, we employ RRKM calculations. The rate equations for the title reaction were derived according to Fig. 14 and solved with the rate constants computed by the RRKM theory. We employed the steady-state approximation to obtain the branching ratios. Table II shows the calculated rate constants for each elementary step in Fig. 14 and the branching ratios at various collision energies. These computations show that **p15** is the major reaction product which contributes at least 76.5% at 19.3 kJmol^{-1} and at least 73% at 38.8 kJmol^{-1} . The contribution of **p14** is in the range of 9%–11% and that of **p16** is less than 1%. Other isomers of C_3H_5 do not play any role in the reaction.

It is interesting to address the possibility of the formation of $C_2H_3+C_3H_3$ in the reaction via intermediate **i5-trans**. Initial calculations showed that the rate constant k_4 for the formation of $C_2H_3+C_3H_3$ is somewhat higher than k_5 for **p14**+H despite the fact that the energetics for the latter is more favorable than for the former. This result is attributed to the fact that at the B3LYP/6-31G** level the transition state for the C–C bond splitting in **i5-trans** has one very low vibrational frequency of 21 cm^{-1} . This leads to very high total number of states for this transition state, which results in the high values for k_4 . The contribution of $C_2H_3+C_3H_3$ is in this case 13.4%–16.6%. However, low vibrational frequencies are usually very sensitive to the theoretical approximation used in calculations. Also, in computations of parti-

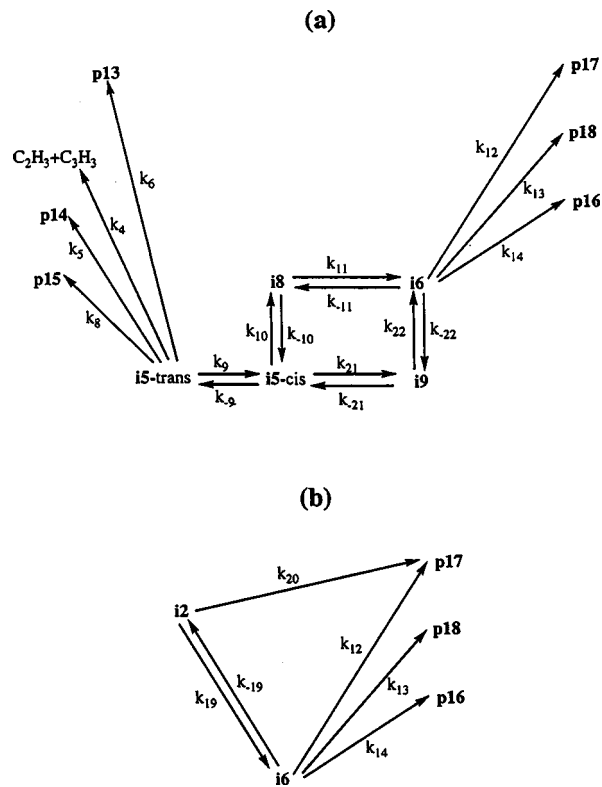


FIG. 14. Diagram showing the reaction pathways included in our RRKM calculations.

tion functions at high temperatures or with large available energies such frequencies should be treated as free or hindered internal rotors rather than as harmonic oscillator. At this stage we estimate possible variations of rate constant k_4 by replacing the lowest vibrational frequency in the transition states by the value of 100 cm^{-1} . Then, we obtain k'_4 which is 4.4 times lower than k_4 and 2.6–3.9 times lower than k_5 (see Table II) for the formation of **p14**, in line with more favorable energy barrier for the latter. Using k'_4 instead k_4 lowers the contribution of $C_2H_3+C_3H_3$ to 3%–4%. We can conclude here that the $C_2H_3+C_3H_3$ channel can play a minor but not insignificant role in the reaction.

We have also calculated the product branching ratios for the case when the cyclic intermediate **i2** is formed in the reaction of the carbon atom with *cis* 1,3-butadiene, cf. Fig. 10. Although this consideration is not directly related to our present experiment, **i2** can be formed in high-temperature combustion flames since 1,3-butadiene is present in its *cis* form as well. We solved the rate equations for the reaction scheme shown in Fig. 14(b) based on the steady-state approximation. The results show that **i2** would produce 95.6% of **p17**, only 4.4% of **p16**, and a negligible amount of **p18**. Again, the most thermodynamically stable **p16** is not the major product because the barrier for H elimination in **i2** is 11.7 kJmol^{-1} lower than the barrier for [1,2] hydrogen migration leading to **i6**, which eventually dissociates to **p16**.

E. Comparison with the reactions of $C(^3P_j)$ with C_2H_4 and C_3H_6

The chemical dynamics and involved potential energy surfaces of reactions of atomic carbon with olefinic mol-

TABLE II. RRKM rate constants in units of s^{-1} as depicted in Figs. 10 and 14, and calculated branching ratios of various reaction products.

Collision energy (kJmol ⁻¹)	0	19.3	28.0	38.8
k_1	1.87×10^3	4.97×10^4	1.45×10^5	4.52×10^5
k_2	1.15×10^5	8.98×10^6	3.48×10^7	1.42×10^8
k_3	5.60×10^{11}	7.25×10^{11}	8.06×10^{11}	9.11×10^{11}
k_4	3.36×10^9	7.88×10^9	1.12×10^{10}	1.68×10^{10}
$k_4'^a$	(7.62×10^8)	(1.78×10^9)	(2.52×10^9)	(3.78×10^9)
k_5	2.97×10^9	5.52×10^9	7.14×10^9	9.66×10^9
k_6	1.02×10^5	3.56×10^5	5.89×10^5	1.05×10^6
k_8	2.61×10^{10}	4.50×10^{10}	5.65×10^{10}	7.38×10^{10}
k_9	8.14×10^{11}	8.77×10^{11}	9.05×10^{11}	9.40×10^{11}
k_{-9}	1.31×10^{12}	1.38×10^{12}	1.41×10^{12}	1.45×10^{12}
k_{10}	3.40×10^8	7.04×10^8	9.50×10^8	1.35×10^9
k_{-10}	7.01×10^8	1.45×10^9	1.95×10^9	2.76×10^9
k_{11}	3.66×10^{10}	4.38×10^{10}	4.72×10^{10}	5.17×10^{10}
k_{-11}	3.16×10^9	4.31×10^9	4.92×10^9	5.76×10^9
k_{12}	7.95×10^7	1.54×10^8	2.04×10^8	2.83×10^8
k_{13}	2.26×10^7	4.55×10^7	6.10×10^7	8.62×10^7
k_{14}	6.33×10^9	8.28×10^9	9.28×10^9	1.06×10^{10}
k_{19}	2.97×10^9	5.13×10^9	6.45×10^9	8.43×10^9
k_{-19}	2.04×10^6	3.97×10^6	5.24×10^6	7.28×10^6
k_{20}	6.41×10^{10}	1.09×10^{11}	1.37×10^{11}	1.78×10^{11}
k_{21}	1.78×10^{10}	2.35×10^{10}	2.64×10^{10}	3.24×10^{10}
k_{-21}	1.13×10^{11}	1.60×10^{11}	1.86×10^{11}	2.21×10^{11}
k_{22}	1.39×10^8	2.65×10^8	3.46×10^8	4.74×10^8
k_{-22}	1.96×10^6	3.92×10^6	5.24×10^6	7.37×10^6
$k(\mathbf{p16})^b$	2.14×10^8	4.38×10^8	5.86×10^8	8.23×10^8
$k(\mathbf{p17})^b$	2.69×10^6	8.17×10^6	1.29×10^7	2.19×10^7
$k(\mathbf{p18})^b$	7.65×10^5	2.41×10^6	3.85×10^6	6.68×10^6
$k(\mathbf{p16})'^c$	2.92×10^9	5.01×10^9	6.26×10^9	8.14×10^9
$k(\mathbf{p17})'^c$	6.41×10^{10}	1.10×10^{11}	1.37×10^{11}	1.78×10^{11}
$k(\mathbf{p18})'^c$	1.04×10^7	2.75×10^7	4.12×10^7	6.60×10^7
Branching ratios ^d (%)				
p13	$3.11(3.38) \times 10^{-4}$	$6.05(6.75) \times 10^{-4}$	$7.81(8.83) \times 10^{-4}$	0.001(0.001)
$C_2H_3 + C_3H_3$	10.3(2.5)	13.4(3.4)	14.8(3.8)	16.6(4.3)
p14	9.1(9.9)	9.4(10.5)	9.5(10.7)	9.6(11.0)
p15	79.9(86.8)	76.5(85.3)	74.9(84.6)	73.0(83.4)
p16	0.7(0.7)	0.7(0.8)	0.8(0.9)	0.8(0.9)
p17	0.008(0.009)	0.014(0.015)	0.017(0.019)	0.022(0.025)
p18	0.002(0.003)	0.004(0.005)	0.005(0.006)	0.007(0.008)
Branching ratios ^e (%)				
p16'	4.4	4.4	4.4	4.4
p17'	95.6	95.6	95.6	95.6
p18'	0.016	0.024	0.029	0.035

^aRate constant k_4 computed with the change of the lowest real vibrational frequency in transition state **t27** from 21 cm^{-1} (B3LYP/6-311G**) to 100 cm^{-1} .

^bRate constants for the formation of the **p16**, **p17**, and **p18** products from intermediate **i5-trans** calculated by solving the kinetic rate equations [see Fig. 14(a)] based on the steady-state approximation.

^cRate constants for the formations of the **p16**, **p17**, and **p18** products from intermediate **i2** in the reaction of $C(^3P_j)$ with cis-1,3-butadiene calculated by solving the kinetic rate equations [see Fig. 14(b)] based on the steady-state approximation.

^dCalculated branching ratios of various products for the reaction proceeding via intermediate **i5-trans**. In parentheses: the values computed using k_4' instead of k_4 .

^eCalculated branching ratios of various products for the reaction proceeding via intermediate **i2**.

ecules such as ethylene and propylene depict common features. The reactions are governed by indirect scattering dynamics and about 30%–35% of the total available energy channels into the translational degrees of freedom. The carbon attack proceeds via complex formation through a barrierless addition of $C(^3P_j)$ to the π electron density. This path-

way yields (substituted) cyclopropylidene intermediates which are stabilized by $210\text{--}270 \text{ kJmol}^{-1}$ with respect to the reactants. All complexes rotate around their C axes and undergo ring opening through barriers between 40 and 60 kJmol^{-1} to form (substituted) triplet allene intermediates. The latter reside in potential energy wells $360\text{--}400 \text{ kJmol}^{-1}$

deep compared to atomic carbon and the olefine. The fate of the triplet allene complexes is governed by H loss channels to (substituted) propargyl radicals via tight exit transition states located about 10–25 kJmol⁻¹ above the products. Most of the initial angular momentum channels into rotational excitation of the products predominantly excited to C-like rotations. The presence of an exit barrier is documented in the center-of-mass translation energy distributions as well as all $P(E_T)$'s peak around 20–50 kJmol⁻¹. The exothermicities to the C₃H₂R (R+CH₃ or C₂H₃) are very similar and range between 200 and 220 kJmol⁻¹. This demonstrates that the substitution of a hydrogen atom in ethylene by a side group has little effect on the energetics of the reaction.

Besides these similarities, there is one striking difference in the reaction of atomic carbon with propylene and 1,3 butadiene. Here, the CH₃ group is conserved in the reaction and acts as a spectator. Although no H atom loss occurs from the C₂H₃ group, the increased stabilization of **p14** versus **p15** demonstrates an enhanced delocalization of the unpaired electron. In addition, if the cis 1,3-butadiene reacts, the side group can be actively involved in the chemistry, since atomic carbon can add to both terminal carbon atoms. Therefore, we cannot regard C₂H₃ as a spectator side group in this case.

VI. COMBUSTION CHEMISTRY APPLICATIONS

Our crossed beam studies showed explicitly that the title reaction leads to 1- and 3-vinylpropargyl radicals, HCCCH–C₂H₃(X²A''), and H₂CCC–C₂H₃(X²A''). This reaction proceeds via an initial addition of C(³P_j) to trans-1,3-butadiene to form a three-membered ring intermediate **i1** followed by ring opening to a substituted triplet allene species **i5** and H atom emission to the products. Although these experiments did not show any evidence of the cyclopentadienyl radical which is thought to be a potential precursor to PAH molecules, the explicit identification of chain C₅H₅ radicals holds far-reaching consequences for combustion processes. Here, Burcat and Dvinyaninov investigated the decomposition pattern of the cyclopentadienyl radical and found HCCCHC₂H₃ as the main decomposition product.³⁵ Based on this finding it can be strongly assumed that in combustion flames HCCCHC₂H₃ can undergo ring closure followed by H atom migration to form the cyclopentadienyl radical once the entrance barrier can be passed via a third body reaction. Likewise, in denser reaction environments such as flames, a collision induced trans-cis isomerization of 1,3-butadiene prior to a C(³P_j) addition can form the cyclopentadienyl radical via **i2** and **i6**.

VII. ASTROPHYSICAL IMPLICATIONS

Besides its potential importance in combustion chemistry, investigating the formation of C₅H₅ isomers is expected to contribute to the modeling of formation of complex molecules in the interstellar space. Here, the PAH synthesis in circumstellar envelopes is of crucial importance since these molecules are considered as the condensation nuclei to form larger carbon-rich grain materials which are considered to be formed in carbon-rich circumstellar shells. Here, the chemi-

cal details leading to large organic molecules are only dimly understood and possibly initiated by a recombination of two pentadienyl radicals, cf. Sec. I. Our proposed mechanism suggests the growth by addition of carbon atoms to unsaturated molecules such as 1,3-butadiene and is supported by recent investigations. Although our crossed beam experiments did not give any proof of a cyclic C₅H₅ isomer, the situation in circumstellar envelopes close to the central carbon star is different from the single collision conditions. Compared to our experiments, the molecular number density is higher, and the C₅H₅ chain can isomerize upon a successive collision to cyclic C₅H₅ isomers. In strong analogy to combustion processes, a collision-induced trans-cis isomerization of 1,3-butadiene can precede the reaction with atomic carbon, and the pentadienyl radical can be formed via **i2** and **i6**.

VIII. CONCLUSIONS

The reaction between ground state carbon atoms, C(³P_j), and 1,3-butadiene, H₂CCHCHCH₂, was studied at averaged collision energies of 19.3, 28.0, and 38.8 kJmol⁻¹ using the crossed molecular beam technique. The carbon atom attacks the π-orbital of the butadiene molecule without a barrier via a loose, reactantlike transition state located at the centrifugal barrier to form a cyclopropylidene derivative. The triplet radical rotates in a plane which is almost perpendicular to the total angular momentum vector **J** around its C-axis undergoing ring opening to a vinyl substituted triplet allene molecule. This complex fragments via two micro-channels through H atom emission to form 1- and 3-vinylpropargyl radicals, HCCCH–C₂H₃(X²A''), and H₂CCC–C₂H₃(X²A''), through tight exit transition states. The unambiguous identification of two chain isomers of C₅H₅ under a single collision represents a further example of a carbon-hydrogen exchange in reactions of ground state carbon atoms with unsaturated hydrocarbons. In denser media such as combustion flames and close to the central star of circumstellar envelopes, the linear isomer can show a ring closure to form cyclic C₅H₅ isomers such as the cyclopentadienyl radical—a postulated intermediate in the formation of PAHs—via HCCCHC₂H₃. Finally, a collision-induced trans-cis isomerization of 1,3-butadiene prior to a C(³P_j) addition can form the pentadienyl radical via cyclic reaction intermediates. The role of cyclic C₅H₅ isomers in these environments will be investigated in future RRKM calculations.

ACKNOWLEDGMENTS

R.I.K. is indebted the Deutsche Forschungsgemeinschaft for a *Habilitation* fellowship (IC1-Ka1081/3-1). This work was supported by Academia Sinica, Taiwan, the National Science Council of R.O.C., and by the Petroleum Research Fund of R.O.C. We are thankful to Dr. A. H. H. Chang for her assistance with RRKM calculations. This work was performed within the international astrophysics network.

¹US Clean Air Act Amendment 1990.

²R. I. Kaiser and K. Roessler, *Astrophys. J.* **475**, 144 (1997), and references therein.

³N. M. Marinov *et al.*, *Combust. Flame* **114**, 192 (1998); N. M. Marinov

- et al.*, *Combust. Sci. Technol.* **116/117**, 211 (1996); N. M. Marinov *et al.*, *ibid.* **128**, 295 (1997).
- ⁴C. Melius *et al.*, *Twenty-sixth Symposium on Combustion/The Combustion Institute* (1996), p. 685.
- ⁵N. M. Marinov *et al.*, *Combust. Sci. Technol.* **128**, 295 (1997).
- ⁶A. M. Mebel and M. C. Lin, *J. Am. Chem. Soc.* **116**, 9577 (1994); M. C. Lin and A. M. Mebel, *J. Phys. Org. Chem.* **8**, 407 (1995); R. Liu, K. Morokuma, A. M. Mebel, and M. C. Lin, *J. Phys. Chem.* **100**, 9314 (1996).
- ⁷W. C. Hung, M. L. Huang, Y. C. Lee, and Y. P. Lee, *J. Chem. Phys.* **103**, 9941 (1995).
- ⁸M. J. Castaldi *et al.*, *Twenty-sixth Symposium on Combustion/The Combustion Institute* (1996), p. 693.
- ⁹Y. T. Lee, J. D. McDonald, P. R. LeBreton, and D. R. Herschbach, *Rev. Sci. Instrum.* **40**, 1402 (1969).
- ¹⁰R. I. Kaiser and A. G. Suits, *Rev. Sci. Instrum.* **66**, 5405 (1995).
- ¹¹G. O. Brink, *Rev. Sci. Instrum.* **37**, 857 (1966).
- ¹²M. S. Weis, Ph.D. thesis, University of California, Berkeley, 1986; M. Vernon, thesis, University of California, Berkeley, 1981.
- ¹³A. D. Becke, *J. Chem. Phys.* **97**, 9173 (1992).
- ¹⁴C. Lee, W. Yang, and R. G. Parr, *Phys. Rev. B* **37**, 785 (1988).
- ¹⁵R. Krishnan, M. Frisch, and J. A. Pople, *J. Chem. Phys.* **72**, 4244 (1988).
- ¹⁶G. D. Purvis and R. J. Bartlett, *J. Chem. Phys.* **76**, 1910 (1982).
- ¹⁷A. M. Mebel, K. Morokuma, and M. C. Lin, *J. Chem. Phys.* **103**, 7414 (1995).
- ¹⁸L. A. Curtiss, K. Raghavachari, and J. A. Pople, *J. Chem. Phys.* **98**, 1293 (1993).
- ¹⁹M. J. Frisch, G. W. Trucks, H. B. Schlegel *et al.*, GAUSSIAN 94, Revision D.4 (Gaussian, Inc., Pittsburgh, PA, 1995).
- ²⁰MOLPRO is a package of *ab initio* programs written by H.-J. Werner and P. J. Knowles, with contributions from J. Almlöf, R. D. Amos, M. J. O. Deegan, S. T. Elbert, C. Hampel, W. Meyer, K. Peterson, R. Pitzer, A. J. Stone, P. R. Taylor, and R. Lindh.
- ²¹J. F. Stanton, J. Gauss, J. D. Watts, W. J. Lauderdale, and R. J. Bartlett, ACES-II, University of Florida.
- ²²A. Mebel *et al.*, *J. Chem. Phys.* (in preparation).
- ²³H. Eyring, S. H. Lin, and S. M. Lin, *Basis Chemical Kinetics* (Wiley, New York, 1980).
- ²⁴Due to a limited budget of our lab, a complete angular distribution could not be recorded. Likewise, no experiments with H₂CCDCDCH₂ could be performed.
- ²⁵W. B. Miller, S. A. Safron, and D. R. Herschbach, *Discuss. Faraday Soc.* **44**, 108,291 (1967); W. B. Miller, Ph.D. thesis, Harvard University, Cambridge, 1969.
- ²⁶R. I. Kaiser, D. Stranges, Y. T. Lee, and A. G. Suits, *J. Chem. Phys.* **105**, 8721 (1996).
- ²⁷R. I. Kaiser, I. Hahndorf, L. C. L. Huang, Y. T. Lee, H. F. Bettinger, P. v. R. Schleyer, and H. F. Schaefer III, *J. Chem. Phys.* **110**, 6091 (1999).
- ²⁸R. I. Kaiser, A. M. Mebel, A. H. H. Chang, S. H. Lin, and Y. T. Lee, *J. Chem. Phys.* **110**, 10330 (1999).
- ²⁹R. I. Kaiser, D. Stranges, H. M. Bevsek, Y. T. Lee, and A. G. Suits, *J. Chem. Phys.* **106**, 4945 (1997).
- ³⁰D. C. Clary, N. Haider, D. Husain, and M. Kabir, *Astrophys. J.* **422**, 416 (1994).
- ³¹NIST database <http://webbook.nist.gov/>
- ³²R. I. Kaiser, C. Ochsenfeld, M. Head-Gordon, Y. T. Lee, and A. G. Suits, *Science* **274**, 1508 (1996).
- ³³R. I. Kaiser, Y. T. Lee, and A. G. Suits, *J. Chem. Phys.* **105**, 8705 (1996).
- ³⁴R. I. Kaiser, W. Sun, A. G. Suits, and Y. T. Lee, *J. Chem. Phys.* **107**, 8713 (1997).
- ³⁵P. Ehrenfreund, B. H. Foing, L. d'Hendecourt, P. Jeniskens, and F. X. Desert, *Astron. Astrophys.* **299**, 213 (1999); M. Frenklach and E. D. Feigelson, *Astrophys. J.* **341**, 372 (1998); G. von Helden, N. G. Gotts, and M. T. Bowers, *Nature (London)* **363**, 60 (1993); J. M. Hunter, J. L. Fye, E. J. Roskamp, and M. F. Jarrold, *J. Phys. Chem.* **98**, 1810 (1994).
- ³⁶G. Scoles, *Atomic and Molecular Beam Data* (Oxford U.P., Oxford, 1992).